

Output feedback control of relative spacecraft attitude

Thomas R. Krogstad Jan Tommy Gravdahl

Department of Engineering Cybernetics, Norwegian University of Science and Technology
Trondheim, Norway

thomas.krogstad@itk.ntnu.no tommy.gravdahl@itk.ntnu.no

Abstract—In this paper we present a controller-observer scheme for relative spacecraft attitude control. The system of interest is a leader-follower formation, where we assume the leader is controlled by some stable controller and we want the follower to track the attitude of the leader. Furthermore we assume that only the relative attitude is available for control purposes, and to estimate the relative angular velocity we introduce an error observer. The resulting closed-loop system is proved to be uniformly practically asymptotically stable to a ball centered at the origin.

I. INTRODUCTION

Coordinated control of autonomous vehicles, e.g. autonomous underwater vehicles, unmanned aerial vehicles, mobile robots and spacecraft is an active area of research [1]–[3], and an enabling technology for a number of relevant applications.

The focus of this paper is the control of relative spacecraft attitude. For a general introduction to attitude control of spacecraft the reader is referred to [4] and [5]. Autonomous control of relative spacecraft motion has received much interest [6]–[9], due in part to several inherent advantages the distributed design adds to a mission. By distributing payload on several spacecraft, redundancy is added to the system, minimizing the risk of total mission failure, several cooperating spacecraft can solve assignments which are more difficult and expensive, or even impossible with a single spacecraft, and the launch costs may be reduced since the spacecraft can be distributed on more inexpensive launch vehicles. A condition for formation flight is however a fully autonomous vehicle, as controlling spacecraft in close formation is only possible using automatic control. This results in stringent requirements on control algorithms and measurement systems.

Examples of planned applications include synthetic aperture radar imaging [10], where the use of a formation can increase the resolution of the gathered data, and space based telescopes where it will be necessary to distribute the functions of the telescope on several vehicles [11].

The contribution of this paper is the design of an observer-controller output feedback scheme for relative spacecraft attitude. The scheme is developed for a leader-follower spacecraft formation, where the leader is assumed to be controlled by an asymptotically stable tracking controller. Furthermore we assume that the follower has knowledge about its own attitude and angular velocity in addition to the relative attitude with respect to the leader. Since we do

not know the angular velocity and acceleration of the leader, we design an error observer in spirit of the work presented in [12].

The paper is organized as follows: In section II we present the system model and some preliminary notation, section III briefly discusses the concept of practical stability, the controller-observer scheme is designed and proved in section IV, while we provide a simulation of a spacecraft formation under autonomous closed-loop control in section V.

II. SYSTEM MODEL

The relative attitude motion of the leader-follower formation is modeled using Euler's momentum equation and the quaternion attitude parameterization of $SO(3)$, using the notation of [13].

A. Kinematics

1) *Coordinate frames*: To represent the attitude of a rotating rigid body we first introduce the concept of coordinate frames. Coordinate frames are given by a set of three orthonormal basis vectors that obey the right hand rule, and which can be considered as a linear operator. In this paper we will consider three such coordinate frames. The ECI or Earth Centered Inertial frame, which is a inertial frame, centered in the earth with a fixed axis toward the sun, and the leader and follower body frames which are fixed in the respective vehicle's center of gravity and coinciding with the principle axis of inertia. In the following we use indexes i , l and f to denote ECI, leader body and follower body frames respectively.

2) *Rotation matrix*: To give the orientation of one coordinate frame relative to another or to transform a vector between frames, we introduce the rotation matrix. Rotation matrices are linear transformations which form the manifold $SO(3)$ defined as

$$SO(3) = \{\mathbf{R} \in \mathbb{R}^{3 \times 3} \text{ s.t. } \det \mathbf{R} = 1, \mathbf{R}^T \mathbf{R} = \mathbf{I}_{3 \times 3}\}. \quad (1)$$

To transform a vector $\mathbf{v} \in \mathbb{R}^3$ between frames a and b we use the notation

$$\mathbf{v}^b = \mathbf{R}_a^b \mathbf{v}^a. \quad (2)$$

3) *Attitude parametrization*: In this paper we parameterize the rotation matrix using the non-minimal, 4-parameter representation known as unit quaternions or Euler parameters. The quaternion corresponding to a rotation between

frames i and j , is given by

$$\mathbf{q}_{ij} = \begin{bmatrix} \eta \\ \boldsymbol{\epsilon} \end{bmatrix} \quad (3)$$

where $\eta \in \mathbb{R}$ and $\boldsymbol{\epsilon} \in \mathbb{R}^3$, and is constrained by $\eta^2 + \boldsymbol{\epsilon}^T \boldsymbol{\epsilon} = 1$. As any rotation can be represented as a rotation ϕ about an axis \mathbf{e} known as the Euler axis, we may define the quaternion as

$$\eta = \cos \frac{\phi}{2} \quad \boldsymbol{\epsilon} = \mathbf{e} \sin \frac{\phi}{2}, \quad (4)$$

with corresponding rotation matrix

$$\mathbf{R}(\mathbf{q}_{ij}) = \mathbf{R}_j^i = (\eta^2 - \boldsymbol{\epsilon}^T \boldsymbol{\epsilon}) \mathbf{I}_{3 \times 3} + 2\boldsymbol{\epsilon} \boldsymbol{\epsilon}^T - 2\eta \mathbf{S}(\boldsymbol{\epsilon}). \quad (5)$$

4) *Quaternion operations:* Quaternion multiplication is denoted \otimes and for two unit quaternions $\mathbf{q}_j = [\eta_j, \boldsymbol{\epsilon}_j^T]^T$, $j \in \{1, 2\}$, it is defined as:

$$\mathbf{q}_1 \otimes \mathbf{q}_2 = \begin{bmatrix} \eta_1 \\ \boldsymbol{\epsilon}_1 \end{bmatrix} \otimes \begin{bmatrix} \eta_2 \\ \boldsymbol{\epsilon}_2 \end{bmatrix} = \begin{bmatrix} \eta_1 \eta_2 - \boldsymbol{\epsilon}_1^T \boldsymbol{\epsilon}_2 \\ \eta_1 \boldsymbol{\epsilon}_2 + \eta_2 \boldsymbol{\epsilon}_1 + \mathbf{S}(\boldsymbol{\epsilon}_1) \boldsymbol{\epsilon}_2 \end{bmatrix}, \quad (6)$$

where $\mathbf{S}(\cdot)$ is the cross-product operator on a row-vector defined as

$$\mathbf{S}(\mathbf{x}) \triangleq \begin{bmatrix} 0 & -x_3 & x_2 \\ x_3 & 0 & -x_1 \\ -x_2 & x_1 & 0 \end{bmatrix}. \quad (7)$$

The quaternion multiplication defined in (6) can also be used to represent composite rotations $\mathbf{R}_c^a = \mathbf{R}_b^a \mathbf{R}_c^b$ as

$$\mathbf{q}_{ac} = \mathbf{q}_{ab} \otimes \mathbf{q}_{bc} \quad (8)$$

Furthermore we have that the inverse quaternion

$$\mathbf{q}_{ab}^{-1} = \begin{bmatrix} \eta \\ -\boldsymbol{\epsilon} \end{bmatrix} \quad (9)$$

corresponds to the reverse rotation of $-\phi$ about \mathbf{e} .

5) *Differential kinematics:* The differential kinematics describes how the attitude of the rigid body evolves on $SO(3)$ and in terms of a rotation matrix it is given by

$$\dot{\mathbf{R}}_j^i = \mathbf{S}(\boldsymbol{\omega}_{ij}^i) \mathbf{R}_j^i = \mathbf{R}_j^i \mathbf{S}(\boldsymbol{\omega}_{ij}^j). \quad (10)$$

where $\boldsymbol{\omega}_{ij}^j$ is the angular velocity of frame j relative to the inertial frame i , given in frame j . When parameterized with the quaternion, the differential kinematics is given by

$$\dot{\mathbf{q}}_{ij} = \frac{1}{2} \mathbf{Q}(\mathbf{q}_{ij}) \boldsymbol{\omega}_{ij}^j, \quad \mathbf{Q}(\mathbf{q}_{ij}) = \begin{bmatrix} -\boldsymbol{\epsilon}^T \\ \eta \mathbf{I}_{3 \times 3} + \mathbf{S}(\boldsymbol{\epsilon}) \end{bmatrix}. \quad (11)$$

In the following, $j = \{l, f\}$, is used to denote the body frames of the leader and follower spacecraft.

B. Kinetics

The kinetic equations, relates the change of angular velocity to angular velocity, disturbances and control torques. In the leader and follower body frame the angular velocity of the vehicle with respect to the inertial coordinates is given by $\boldsymbol{\omega}_{il}^l$ and $\boldsymbol{\omega}_{if}^f$ respectively. The differential equations according to Euler's momentum equation are given as

$$\dot{\boldsymbol{\omega}}_{ij}^j = \mathbf{S}(\mathbf{J}_j \boldsymbol{\omega}_{ij}^j) \boldsymbol{\omega}_{ij}^j + \boldsymbol{\tau}_j, \quad (12)$$

where $j \in \{l, f\}$, i denotes the inertial frame, \mathbf{J}_j is the respective vehicle's moment of inertia matrix and $\boldsymbol{\tau}_j$ is the control input.

III. PRACTICAL STABILITY

In this section we give a short introduction to the concept of practical stability [1], [14], [15]. This a concept which is of interest in systems with boundedness properties, where we in addition have an attractive domain that depends on system parameters. Similar to the semi-global property where one may arbitrarily increase the region of attraction by increasing the controller gains, one may define a *practical stability* property, which allows for arbitrarily diminishing the size of the non-attractive domain by arbitrarily increasing the parameters in the system.

We denote by $\|\cdot\|$ the Euclidean norm of a vector and the induced \mathcal{L}_2 -norm of matrix. We denote by \mathcal{B}_δ the closed ball in \mathbb{R}^n of radius δ , i.e. $\mathcal{B}_\delta \triangleq \{\mathbf{x} \in \mathbb{R}^n \mid \|\mathbf{x}\| \leq \delta\}$. A continuous function $\alpha : \mathbb{R}_{\geq 0} \rightarrow \mathbb{R}_{\geq}$ is said to be of class \mathcal{K} ($\alpha \in \mathcal{K}$) if it is strictly increasing and $\alpha(0) = 0$. A continuous function $\sigma : \mathbb{R}_{\geq 0} \rightarrow \mathbb{R}_{\geq}$ is of class \mathcal{L} ($\sigma \in \mathcal{L}$) if it is strictly decreasing and $\sigma(s) \rightarrow 0$ as $s \rightarrow \infty$.

Definition 1 (Uniform practical asymptotic stability [1]):

Consider the parameterized nonlinear system

$$\dot{\mathbf{x}} = \mathbf{f}(t, \mathbf{x}, \boldsymbol{\theta}), \quad (13)$$

where $\mathbf{f}(t, \mathbf{x}, \boldsymbol{\theta}) : \mathbb{R}_{\geq 0} \times \mathbb{R}^n \times \mathbb{R}^m \rightarrow \mathbb{R}^n$ is locally Lipschitz in \mathbf{x} and piecewise continuous in t for all $\boldsymbol{\theta}$ under consideration, the following stability consideration is used:

Let $\Theta \subset \mathbb{R}^m$ be a set of parameters. The system in (13) is said to be uniformly practically asymptotically stable (UPAS) on Θ if, given any $\Delta > \delta > 0$ such that $\mathcal{B}_\Delta \subseteq \mathbb{D} \subset \mathbb{R}^n$, there exists $\boldsymbol{\theta}^* \in \Theta$ s.t. for $\dot{\mathbf{x}} = \mathbf{f}(t, \mathbf{x}, \boldsymbol{\theta}^*)$ the ball \mathcal{B}_δ is uniformly asymptotically stable on \mathcal{B}_Δ .

The following corollary was given in [1], and applies to the practical stability analysis of systems with a Lyapunov function that can be upper and lower bounded by a polynomial function.

Corollary 1: Let $\sigma_i : \mathbb{R}^m \rightarrow \mathbb{R}_{\geq 0}$, $i \in \{1, \dots, N\}$, be continuous functions, positive over Θ , and let \underline{a} , \bar{a} , q and Δ be positive constants. Assume that, for any $\boldsymbol{\theta} \in \Theta$, there exists a continuously differentiable Lyapunov function $V : \mathbb{R}_{\geq 0} \times \mathbb{D} \rightarrow \mathbb{R}_{\geq 0}$ satisfying, for all $\mathbf{x} \in \mathbb{D}$ and all $t \geq 0$,

$$\underline{a} \min \{\sigma_i(\boldsymbol{\theta})\} \|\mathbf{x}\|^q \leq V(t, \mathbf{x}) \leq \bar{a} \max \{\sigma_i(\boldsymbol{\theta})\} \|\mathbf{x}\|^q. \quad (14)$$

Assume also that for any $\delta \in (0, \Delta)$, there exists a parameter $\boldsymbol{\theta}^*(\delta) \in \Theta$ and a class \mathcal{K} function α_δ such that, for all $\|\mathbf{x}\| \in [\delta, \Delta]$ and all $t \geq 0$,

$$\frac{\partial V}{\partial t}(t, \mathbf{x}) + \frac{\partial V}{\partial \mathbf{x}}(t, \mathbf{x}) \mathbf{f}(t, \mathbf{x}, \boldsymbol{\theta}^*) \leq -\alpha_\delta(\|\mathbf{x}\|). \quad (15)$$

Assume also that for all $i \in \{1, \dots, N\}$,

$$\lim_{\delta \rightarrow 0} \sigma_i(\boldsymbol{\theta}^*(\delta)) \delta^q = 0 \quad \lim_{\delta \rightarrow 0} \sigma_i(\boldsymbol{\theta}^*(\delta)) \neq 0. \quad (16)$$

Then, the system $\dot{\mathbf{x}} = \mathbf{f}(t, \mathbf{x}, \boldsymbol{\theta})$ is UPAS on the parameter set Θ . Moreover, when $\delta = 0$ and the parameter $\boldsymbol{\theta}^*$ is independent of δ , the conditions in (16) are no longer required, and the system $\dot{\mathbf{x}} = \mathbf{f}(t, \mathbf{x}, \boldsymbol{\theta})$ is UAS.

Note that the domain defined by \mathcal{B}_δ in the above corollary, can be arbitrarily diminished.

IV. CONTROL AND OBSERVER DESIGN

In this paper we have assumed that the available measurements are the orientation and angular velocity of the follower and the relative orientation with respect to the leader. Furthermore we assume that the angular acceleration and angular velocity of the leader vehicle are bounded.

The control objective is for the follower to track the attitude motion of the leader, expressed as

$$\lim_{t \rightarrow \infty} \boldsymbol{\omega}_e = \mathbf{0} \quad (17)$$

$$\lim_{t \rightarrow \infty} \mathbf{q}_e = [1, 0, 0, 0]^T, \quad (18)$$

where $\boldsymbol{\omega}_e$ and \mathbf{q}_e are relative angular velocity and orientation respectively, defined by

$$\boldsymbol{\omega}_e \triangleq \boldsymbol{\omega}_{if}^f - (\mathbf{R}_f^l)^T \boldsymbol{\omega}_{il}^l, \quad (19)$$

$$\mathbf{q}_e \triangleq \mathbf{q}_{il}^{-1} \otimes \mathbf{q}_{if}. \quad (20)$$

where $\boldsymbol{\omega}_{il}^l$ and $\boldsymbol{\omega}_{if}^f$ are leader and follower angular velocities respectively, and \mathbf{R}_f^l is the rotation matrix corresponding to the relative attitude error \mathbf{q}_e as defined in (5).

We define a synchronization measure

$$\mathbf{s} \triangleq \boldsymbol{\omega}_e + \lambda \boldsymbol{\epsilon}_e. \quad (21)$$

Moreover, we define a virtual reference trajectory for the follower spacecraft as

$$\boldsymbol{\omega}_r = (\mathbf{R}_f^l)^T \boldsymbol{\omega}_{il}^l - \lambda \boldsymbol{\epsilon}_e, \quad (22)$$

enabling us to rewrite the synchronization measure as

$$\mathbf{s} = \boldsymbol{\omega}_{if}^f - \boldsymbol{\omega}_r. \quad (23)$$

We can now write the system dynamics as

$$\mathbf{J}_f \dot{\mathbf{s}} = \mathbf{S} \left(\mathbf{J}_f \boldsymbol{\omega}_{if}^f \right) \boldsymbol{\omega}_{if}^f + \boldsymbol{\tau} - \mathbf{J}_f \dot{\boldsymbol{\omega}}_r \quad (24a)$$

$$\dot{\mathbf{q}}_e = \frac{1}{2} \mathbf{Q}(\mathbf{q}_e) (\mathbf{s} - \lambda \boldsymbol{\epsilon}_e) \quad (24b)$$

Proposition 1: *The system (24a)-(24b), with the control input defined as*

$$\boldsymbol{\tau}_f = -k_d \mathbf{s} - k_p \boldsymbol{\epsilon}_e + \mathbf{J}_f \dot{\boldsymbol{\omega}}_r - \mathbf{S} \left(\mathbf{J}_f \boldsymbol{\omega}_{if}^f \right) \boldsymbol{\omega}_{if}^f, \quad (25)$$

where $k_d \in \mathbb{R}_{>0}$ and $k_p \in \mathbb{R}_{>0}$ are constants, has a locally uniformly exponentially stable (ULES) origin $(\mathbf{s}, \boldsymbol{\epsilon}_e) = (0, 0)$. From (21) which we can conclude exponential convergence of the relative attitude and orientation errors as defined in (17) and (18).

Proof: The proof can be carried out using the radially unbounded, positive definite Lyapunov function

$$V = \frac{1}{2} \mathbf{s}^T \mathbf{J}_f \mathbf{s} - 2k_p(1 - \eta_e), \quad (26)$$

which has time-derivative along the trajectories

$$\dot{V} = -k_d \mathbf{s}^T \mathbf{s} - k_p \lambda \boldsymbol{\epsilon}_e^T \boldsymbol{\epsilon}_e < 0, \quad (27)$$

which is negative definite. Hence we can conclude ULES of the system origin. ■

Remark 1: *It was shown in [16] that it is not possible to achieve a global attitude control using continuous feedback. And one may experience the unwinding phenomenon, ie. due*

to dual equilibrium points in the dynamics, corresponding to the same physical attitude, one of which is unstable, the vehicle which initialized at the correct way, after an perturbation, rotate 2π about some axis.

As the relative angular velocity is not available, the controller in Proposition 1 cannot be implemented. Inspired by [12], [17], we therefore design an error-observer to estimate the synchronization measure using the measured relative attitude.

We define the error-variables

$$\tilde{\mathbf{s}} \triangleq \mathbf{s} - \hat{\mathbf{s}} \quad (28)$$

$$\tilde{\mathbf{q}}_e \triangleq \mathbf{q}_e^{-1} \otimes \hat{\mathbf{q}}_e, \quad (29)$$

where $\hat{\mathbf{s}}$ is the estimate of the synchronization measure and $\hat{\mathbf{q}}_e$ is the estimate of the relative attitude. The observer is implemented as

$$\mathbf{J}_f \dot{\hat{\mathbf{s}}} = \mathbf{S} \left(\mathbf{J}_f \boldsymbol{\omega}_{if}^f \right) \boldsymbol{\omega}_{if}^f + \boldsymbol{\tau}_f - l_2 \tilde{\boldsymbol{\epsilon}}_e \quad (30)$$

$$\dot{\hat{\mathbf{q}}}_e = \frac{1}{2} \mathbf{Q}(\hat{\mathbf{q}}_e) (\tilde{\mathbf{R}}_e^T (\hat{\mathbf{s}} - \lambda \boldsymbol{\epsilon}) - l_1 \tilde{\boldsymbol{\epsilon}}_e), \quad (31)$$

which imply that the observer error dynamics can be written as

$$\mathbf{J} \dot{\tilde{\mathbf{s}}} = -\mathbf{J} \dot{\boldsymbol{\omega}}_r + l_2 \tilde{\boldsymbol{\epsilon}}_e \quad (32a)$$

$$\dot{\tilde{\mathbf{q}}} = \frac{1}{2} \mathbf{Q}(\tilde{\mathbf{q}}_e) (-\tilde{\mathbf{R}}_e^T \tilde{\mathbf{s}} - l_1 \tilde{\boldsymbol{\epsilon}}_e). \quad (32b)$$

Proposition 2: *The system dynamics obtained by combining (24) and (32), and defining the control input of the follower as*

$$\boldsymbol{\tau} = -\mathbf{S} \left(\mathbf{J}_f \boldsymbol{\omega}_{if}^f \right) \boldsymbol{\omega}_{if}^f - k_p \boldsymbol{\epsilon}_e - k_d \hat{\mathbf{s}}, \quad (33)$$

is UPAS. In addition since $\mathbf{s} = 0$ and $\boldsymbol{\epsilon}_e = 0$ corresponds to $\boldsymbol{\omega}_e = 0$, we can conclude UPAS of the relative attitude and angular velocity.

Proof: The stability proof is conducted using the Lyapunov function

$$V = \frac{1}{2} \mathbf{s}^T \mathbf{J}_f \mathbf{s} + \frac{1}{2} \tilde{\mathbf{s}}^T \mathbf{J}_f \tilde{\mathbf{s}} - c \mathbf{s}^T \mathbf{J}_f \tilde{\mathbf{s}} + 2k_p(1 - \eta_e) + 2l_1(1 - \tilde{\eta}_e), \quad (34)$$

which is positive definite and radially unbounded for $0 < c < 1$. Taking the time derivative along the system trajectories we obtain

$$\dot{V} = -\boldsymbol{\chi}^T \mathbf{Q} \boldsymbol{\chi} + \Delta_\omega, \quad (35)$$

where

$$\mathbf{Q} = \begin{bmatrix} k_d \mathbf{I} & \mathbf{0} & -\frac{1}{2} k_d c \mathbf{I} & \frac{1}{2} c l_2 \mathbf{I} \\ \mathbf{0} & k_p \lambda \mathbf{I} & \frac{1}{2} c k_p \mathbf{I} & \mathbf{0} \\ -\frac{1}{2} k_d c \mathbf{I} & \frac{1}{2} c k_p \mathbf{I} & c k_d \mathbf{I} & \frac{1}{2} (l_1 \tilde{\mathbf{R}}_e - l_2 \mathbf{I}) \\ \frac{1}{2} c l_2 \mathbf{I} & \mathbf{0} & \frac{1}{2} (l_1 \tilde{\mathbf{R}}_e^T - l_2 \mathbf{I}) & l_1^2 \end{bmatrix} \quad (36)$$

and

$$\boldsymbol{\chi} \triangleq \begin{bmatrix} \mathbf{s} \\ \boldsymbol{\epsilon}_e \\ \tilde{\mathbf{s}} \\ \tilde{\boldsymbol{\epsilon}}_e \end{bmatrix}. \quad (37)$$

We reorganize the terms in \dot{V} to be able to see which gains result in a positive definite \mathbf{Q}

$$\begin{aligned} \dot{V} = & -\frac{1}{2} \begin{bmatrix} \mathbf{s} \\ \tilde{\mathbf{s}} \end{bmatrix}^T \underbrace{\begin{bmatrix} k_d \mathbf{I} & -k_d c \mathbf{I} \\ -k_d c \mathbf{I} & \frac{2}{3} k_d c \mathbf{I} \end{bmatrix}}_{\mathbf{Q}_1} \begin{bmatrix} \mathbf{s} \\ \tilde{\mathbf{s}} \end{bmatrix} \\ & -\frac{1}{2} \begin{bmatrix} \boldsymbol{\epsilon}_e \\ \tilde{\boldsymbol{\epsilon}}_e \end{bmatrix}^T \underbrace{\begin{bmatrix} k_p \lambda \mathbf{I} & \mathbf{0} \\ \mathbf{0} & \frac{2}{3} l_1^2 \mathbf{I} \end{bmatrix}}_{\mathbf{Q}_2} \begin{bmatrix} \boldsymbol{\epsilon}_e \\ \tilde{\boldsymbol{\epsilon}}_e \end{bmatrix} \\ & -\frac{1}{2} \begin{bmatrix} \mathbf{s} \\ \tilde{\boldsymbol{\epsilon}}_e \end{bmatrix}^T \underbrace{\begin{bmatrix} k_d \mathbf{I} & c l_2 \mathbf{I} \\ c l_2 \mathbf{I} & \frac{2}{3} l_1^2 \mathbf{I} \end{bmatrix}}_{\mathbf{Q}_3} \begin{bmatrix} \mathbf{s} \\ \tilde{\boldsymbol{\epsilon}}_e \end{bmatrix} \\ & -\frac{1}{2} \begin{bmatrix} \tilde{\mathbf{s}} \\ \boldsymbol{\epsilon}_e \end{bmatrix}^T \underbrace{\begin{bmatrix} \frac{2}{3} c k_d \mathbf{I} & c k_p \mathbf{I} \\ c k_p \mathbf{I} & k_p \lambda \mathbf{I} \end{bmatrix}}_{\mathbf{Q}_4} \begin{bmatrix} \tilde{\mathbf{s}} \\ \boldsymbol{\epsilon}_e \end{bmatrix} \\ & -\frac{1}{2} \begin{bmatrix} \tilde{\mathbf{s}} \\ \tilde{\boldsymbol{\epsilon}}_e \end{bmatrix}^T \underbrace{\begin{bmatrix} \frac{2}{6} c k_d \mathbf{I} & -l_2 \mathbf{I} \\ -l_2 \mathbf{I} & \frac{2}{6} l_1^2 \mathbf{I} \end{bmatrix}}_{\mathbf{Q}_5} \begin{bmatrix} \tilde{\mathbf{s}} \\ \tilde{\boldsymbol{\epsilon}}_e \end{bmatrix} \\ & -\frac{1}{2} \begin{bmatrix} \tilde{\mathbf{s}} \\ \tilde{\boldsymbol{\epsilon}}_e \end{bmatrix}^T \underbrace{\begin{bmatrix} \frac{2}{6} c k_d \mathbf{I} & l_1 \tilde{\mathbf{R}}_e \\ l_1 \tilde{\mathbf{R}}_e^T & \frac{2}{6} l_1^2 \mathbf{I} \end{bmatrix}}_{\mathbf{Q}_5} \begin{bmatrix} \tilde{\mathbf{s}} \\ \tilde{\boldsymbol{\epsilon}}_e \end{bmatrix} + \Delta_\omega. \quad (38) \end{aligned}$$

By examining the determinant of the matrices \mathbf{Q}_i find the following conditions on the controller and observer gains, and the Lyapunov function parameters

$$c < \frac{2}{3} \quad (39)$$

$$k_d > \max \left\{ \frac{9l_2^2}{cl_1^2}, 9c, \frac{3ck_p}{2\lambda} \right\} \quad (40)$$

for which V is positive definite and radially unbounded, and \mathbf{Q} is a positive definite matrix.

Furthermore, using bounds on Δ_ω derived in (46) in the Appendix, we rewrite the Lyapunov function derivative as

$$\dot{V} \leq -q_m \|\boldsymbol{\chi}\|^2 + c_1 \|\boldsymbol{\chi}\|^2 + c_2 \|\boldsymbol{\chi}\|, \quad (41)$$

where q_m is the smallest eigenvalue of \mathbf{Q} . Note that q_m can be adjusted by appropriately selecting the controller and observer gains. By restricting the norm of the system state to $\|\boldsymbol{\chi}\| \geq \delta$, we obtain

$$\dot{V} \leq -\frac{1}{2} q_m \|\boldsymbol{\chi}\|^2 - \left(\frac{1}{2} q_m - \frac{c_1}{\delta} - c_2 \right) \|\boldsymbol{\chi}\|^2. \quad (42)$$

Which, when constricting the controller observer gains such that

$$\frac{1}{2} q_m \geq \frac{c_1}{\delta} + c_2 \quad (43)$$

we obtain

$$\dot{V} \leq -\frac{1}{2} q_m \|\boldsymbol{\chi}\|^2, \quad (44)$$

for all $\|\boldsymbol{\chi}\| \in \mathbb{D}$ s.t. $\|\boldsymbol{\chi}\| \geq \delta$. And we can conclude UPAS of the closed loop system as defined in definition 1, according to Corollary 1. ■

V. SIMULATION

In this section a leader-follower spacecraft formation is simulated using the proposed observer-controller structure. The model properties, along with controller and observer gains can be found in table I.

TABLE I
MODEL PARAMETERS

Parameter	Value
Inertia matrix leader	diag{1, 3, 4} [kgm ²]
Inertia matrix follower	diag{10, 3, 4} [kgm ²]
Initial angular velocity leader	[0.1, 0, 0] ^T [raq/s]
Initial angular velocity follower	[0, 0, 0] ^T [rad/s]
Initial orientation	[-1, 0, 0, 0] ^T
Initial orientation	[0.5, 0.5, 0.5, 0.5] ^T
[k _p , k _d , l ₁ , l ₂ , λ]	[700, 4000, 0.5, 120, 1000]

The leader is controlled by an exponentially stable tracking controller, and commanded to do a slew maneuver. After the initialization of the simulation, the leader is perturbed by torque inputs of 10[mN] every 35 seconds.

A. Results

As one can see from fig. 1 and 2, both the synchronization measure and the observer error approach a ball about the origin, which corresponds well with the theoretical findings. Moreover, fig. 3. and 4. show that we also have UPAS for the observer error dynamics. While fig. 5 show that the relative angular velocity also converges.

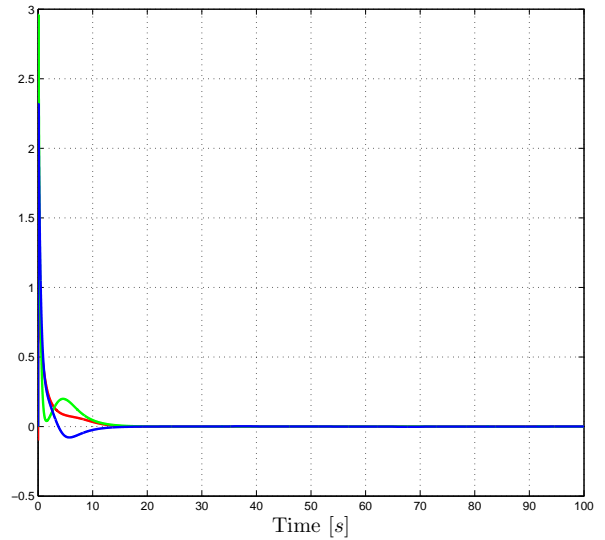


Fig. 1. Synchronization measure s .

VI. CONCLUSION

In this paper we have considered the problem of controlling the relative attitude in a leader-follower spacecraft formation. A controller-observer output feedback approach has been proposed, which guarantees that the relative attitude

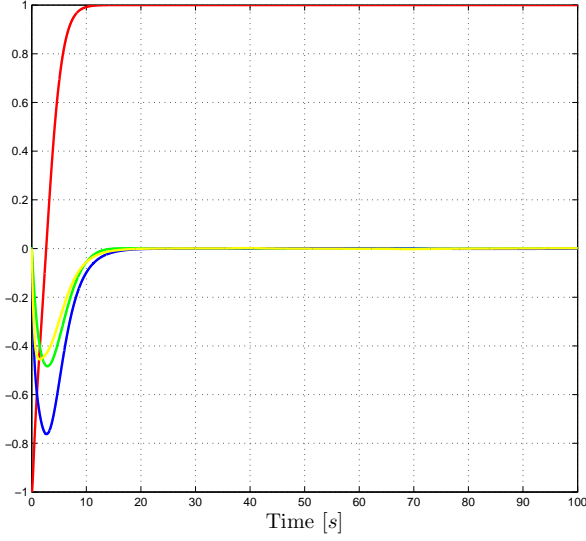


Fig. 2. Attitude synchronization error \mathbf{q}_e .

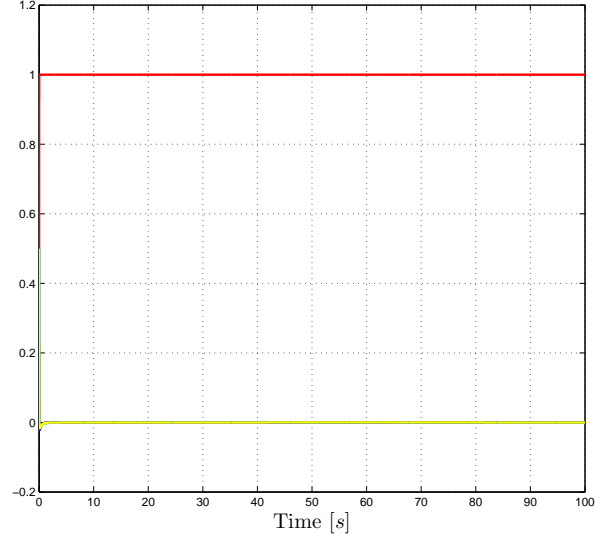


Fig. 4. Observer attitude error $\tilde{\mathbf{q}}$.

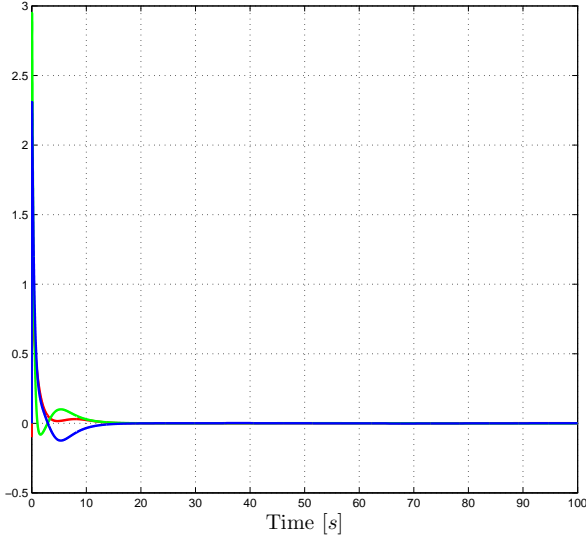


Fig. 3. Observer error $\tilde{\mathbf{s}}$.

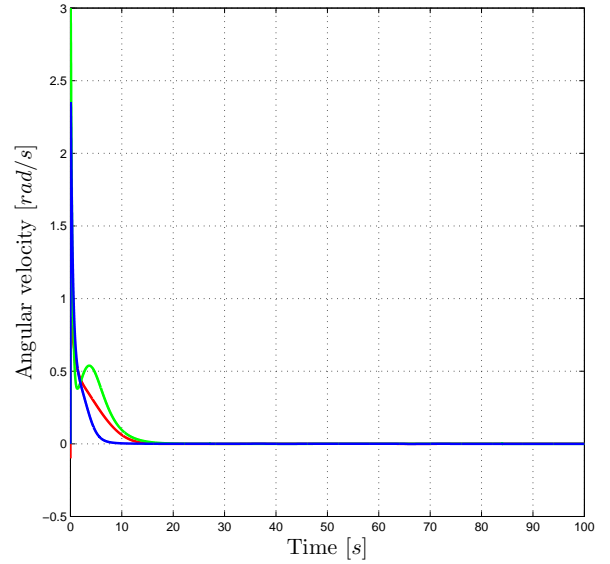


Fig. 5. Angular velocity synchronization error.

converge to a ball about the origin, and that the closed-loop system is uniformly practically asymptotically stable. The performance of the proposed scheme has been investigated through numerical simulations in MATLAB SIMULINK.

APPENDIX

A. Bound on Δ_ω

In this appendix we give the calculation of the bound on Δ_ω

$$\Delta_\omega = \chi^T \begin{bmatrix} -\mathbf{J}\dot{\boldsymbol{\omega}}_r \\ 0 \\ -\mathbf{J}\dot{\boldsymbol{\omega}}_r \\ 0 \end{bmatrix} \quad (45)$$

and

$$\|\Delta_\omega\| \leq 2\|\chi\|\|\mathbf{J}\dot{\boldsymbol{\omega}}_r\| \quad (46)$$

where

$$\mathbf{J}_f \dot{\boldsymbol{\omega}}_r = \mathbf{J}_f (\dot{\mathbf{R}}_f^l)^T \boldsymbol{\omega}_{il}^l + \mathbf{J}_f (\mathbf{R}_f^l)^T \dot{\boldsymbol{\omega}}_{il}^l - \lambda \mathbf{J}_f \dot{\boldsymbol{\epsilon}}_e \quad (47)$$

$$= -\mathbf{J}_f \mathbf{S} (\mathbf{s} - \lambda \boldsymbol{\epsilon}_e) (\mathbf{R}_f^l)^T \boldsymbol{\omega}_{il}^l + \mathbf{J}_f (\mathbf{R}_f^l)^T \dot{\boldsymbol{\omega}}_{il}^l \quad (48)$$

$$+ \lambda^2 \eta_e \mathbf{J}_f \boldsymbol{\epsilon}_e - \lambda \mathbf{J}_f (\eta_e \mathbf{I} + \mathbf{S}(\boldsymbol{\epsilon}_e)) \mathbf{s} \quad (49)$$

Using the bounds on the leader angular velocities and angular acceleration, we obtain

$$\|\mathbf{J}_f \dot{\boldsymbol{\omega}}_r\| \leq c_1 \|\chi\| + c_2 \quad (50)$$

where the constants c_1 and c_2 are given by

$$c_1 = 6\sqrt{3}j_m\beta_l + 3\lambda j_m + \lambda^2 j_m \quad (51)$$

$$c_2 = 3\sqrt{3}j_m\beta_{al} \quad (52)$$

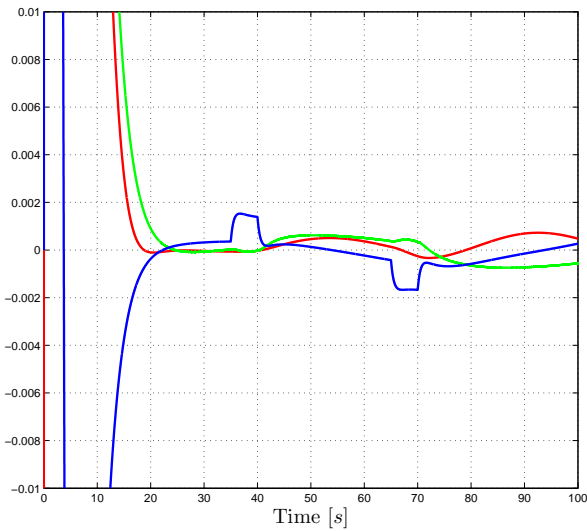


Fig. 6. Zoom in of the synchronization measure plot in fig. 1. Here one can see that the error converges and stays within a δ -ball centered at the origin.

and we have used $\|\omega_{il}^l\| \leq \beta_l$, $\|\dot{\omega}_{il}^l\| \leq \beta_{al}$, $\|\mathbf{J}_f\| \leq j_m$, $\|(\mathbf{R}_f^l)^T\| \leq 3\sqrt{3}$, $\|\eta_e \mathbf{I} + \mathbf{S}(\epsilon_e)\| \leq 3$.

REFERENCES

- [1] R. Kristiansen, "Dynamic synchronization of spacecraft: Modeling and coordinated control of leader-follower spacecraft formations," Ph.D. dissertation, Norwegian University of Science and Technology and Narvik University College, Narvik, Norway, 2008.
- [2] E. Børhaug, A. Pavlov, and K. Pettersen, "Cross-track formation control of underactuated surface vessels," in *Decision and Control, 2006 45th IEEE Conference on*, 2006, pp. 5955–5961.
- [3] H. Nijmeijer and A. Rodriguez-Angeles, *Synchronization of Mechanical Systems*, L. Chua, Ed. Singapore: World Scientific, 2003.
- [4] P. C. Hughes, *Spacecraft attitude dynamics*. New York: John Wiley & Sons, 1986.
- [5] T.-Y. J. Wen and K. Kreutz-Delgado, "The attitude control problem," *IEEE Transactions on Automatic Control*, vol. 36, no. 10, pp. 1148–1162, October 1991.
- [6] R. W. Beard, J. R. T. Lawton, and F. Y. Hadaegh, "A coordination architecture for formation control," *IEEE Transactions on Control Systems Technology*, vol. 9, pp. 777–790, 2001.
- [7] W. Ren and R. W. Beard, "Formation feedback control for multiple spacecraft via virtual structures," in *2004 IEEE Proceedings of Control Theory Application*, 2004.
- [8] H. Pan and V. Kapila, "Adaptive nonlinear control for spacecraft formation flying with coupled translational and attitude dynamics," in *Proceedings of the 40th IEEE Conference on Decision and Control*, 2001.
- [9] W. Kang and H. Yeh, "Co-ordinated attitude control of multi-satellite systems," *International Journal of Robust and Nonlinear Control*, vol. 12, pp. 185–205, 2002.
- [10] A. Moreira, G. Krieger, I. Hajnsek, M. Werner, S. Riegger, and E. Settelmeier, "TanDEM-x: a terraSAR-X add-on satellite for single-pass sar interferometry," in *Proceedings of the 2004 IEEE International Geoscience and Remot Sensing Symposium*, vol. 2, 2004, pp. 1000–1003.
- [11] C. V. M. Fridlund, "DARWIN - The infrared space interferometry mission," *ESA Bulletin*, vol. 100, pp. 20–25, 2000.
- [12] E. Kyrkjebø, "Leader-follower synchronization control of euler-lagrange systems with leader position measurements only," in *Proc. Mediterranean Conf. on Control and Automation*, Athens, Greece, 2007.
- [13] O. Egeland and J. T. Gravdahl, *Modeling and Simulation for Automatic Control*. Trondheim: Marine Cybernetics, 2002.
- [14] W. Hahn, *Stability of Motion*. Springer-Verlag, 1967.

- [15] A. Chaillet, "On stability and robustness of nonlinear systems: Application to cascaded systems," Ph.D. dissertation, UFR Scientifique D'Orsay, Paris, France, 2006.
- [16] S. P. Bhat and D. S. Bernstein, "Topological obstruction to continuous global stabilization of rotational motion and the unwinding phenomenon," *Systems & Control Letters*, vol. 39, no. 1, pp. 63–70, Jan. 2000.
- [17] E. Kyrkjebø, "Motion coordination of mechanical systems: Leader-follower synchronization of euler-lagrange systems using output feedback control," Ph.D. dissertation, Norwegian University of Science and Technology, 2007.